Journal of Cleaner Production 448 (2024) 141749

Contents lists available at ScienceDirect

Journal of Cleaner Production

journal homepage: www.elsevier.com/locate/jclepro

Technical analysis of a novel economically mixed CO_2-Water enhanced geothermal system

Zhenqian Xue [a], Haoming Ma [a,**], Zhe Sun [a], Chengang Lu [b], Zhangxin Chen [a,c,d,*]

[a] Department of Chemical & Petroleum Engineering, University of Calgary, 2500 University Drive NW, Calgary, Alberta, T2N 1N4, Canada
[b] School of Energy Resources, China University of Geosciences (Beijing), Beijing, 100083, China
[c] Eastern Institute of Technology (tentative), Ningbo, 315200, China
[d] National Key Laboratory of Petroleum Resources and Engineering, China University of Petroleum (Beijing), Beijing, 102249, China

ARTICLE INFO

Handling Editor: Panos Seferlis

Keywords:
Enhanced geothermal system
CO_2-Water mixture
Carbon storage
Carbon credit
Net present value

ABSTRACT

Geothermal energy has undoubtedly been considered a promising low-carbon resource in future energy supply responding to the rising energy demand and severe climate concerns. CO_2 has been demonstrated as a comparable alternative for water in developing an Enhanced geothermal system (EGS), which simultaneously unlocks the potential to sequester CO_2 against climate concerns. However, an earlier thermal breakthrough is always observed owing to higher mobility in geothermal reservoirs for CO_2-EGS, and an expensive cost of CO_2 consumption makes CO_2-EGS challenging to achieve economic profitability. In this study, a novel CO_2-water-EGS is proposed to investigate the feasibility of solving the obstacles in conventional EGSs. An integrated analysis for multiple EGS scenarios is carried out from both the technical and economic perspectives. The effects of a CO_2-water ratio, an injection rate and a flow scheme are comprehended. Followed by the determination of an optimal operating strategy. In the results, by reasonably selecting a CO_2 mass ratio and an injection rate, CO_2-water-EGS can recover more geothermal energy and earn more profits than water-EGS and CO_2-EGS. The injection rate shows positive correlations to heat mining, carbon storage, and economic performance, while the impact of a flow scheme is negligible when the total volume of injected fluids remains consistent. From the optimization study, the CO_2-water-EGS with the 110 kg/s injection rate and 20%wt CO_2 ratio shows the highest Net Present Value (NPV) of 42.4 M$. This study proposes theoretical guidance to operators in their decision-making processes on the development of CO_2-water-EGS.

1. Introduction

In response to global warming and increasing energy demand, renewable alternatives are sustainably necessitated for traditional fossil fuels and can fulfill the energy demand and mitigate climate concerns (Anderson and Rezaie, 2019; Yang et al., 2024). Geothermal energy is a well-accepted subsurface renewable resource for providing an abundant energy supply, which can be suitable for the supply of electric power and direct energy harvesting (i.e., heating and cooling applications in buildings). Currently, the power generation from geothermal energy has played a significant role in some countries, for example, Kenya (44%), Iceland (27%), EI Salvador (26%) and New Zealand (18%) of electricity installed capacity (Kabeyi, 2019). In addition, benefiting from its low-carbon intensity, geothermal energy is also acknowledged as one of the most effective strategies to achieve the decarbonization goal. It has been estimated that over one billion tons of carbon emissions can be mitigated by 2050 through the development of geothermal energy (Soltani et al., 2021).

There are several types of geothermal resources, such as hydrothermal, liquid/hot water dominated reservoirs, geo-pressurized geothermal reservoirs, sedimentary basin geothermal resources and hot dry rock (HDR) (Kabeyi, 2019). Among them, HDR shows the potential to convert harvested heat to electricity (Lu, 2018), and an enhanced geothermal system (EGS) is typically deployed to extract heat energy from HDR due

Abbreviations: EGS, Enhanced geothermal system; HDR, Hot dry rock; NPV, Net Present Value; CAPEX, Capital expenditure; OPEX, Operating expenses; CMG, Computer Modelling Group; O&M, Operation and maintenance; CPG, CO2 plume geothermal; IRC, Internal Revenue Code.

* Corresponding author. Department of Chemical & Petroleum Engineering, University of Calgary, 2500 University Drive NW, Calgary, Alberta, T2N 1N4, Canada.
** Corresponding author.
E-mail addresses: haoming.ma@ucalgary.ca (H. Ma), zhachen@ucalgary.ca (Z. Chen).

https://doi.org/10.1016/j.jclepro.2024.141749
Received 3 November 2023; Received in revised form 8 March 2024; Accepted 10 March 2024
Available online 11 March 2024

to its low permeability and porosity (Aghahosseini and Breyer, 2020). In an EGS development, different heat transmission fluids have been studied and used. Water is widely adopted owing to its large heat capacity and thermal stability (Xue and Chen, 2023a). Existing works showed that produced water can even reach a temperature of approximately 200 °C from a 218 °C HDR, which can be subsequently utilized as the working fluid for a geothermal power plant (Lei et al., 2020). Recently, the CO_2-EGS has been suggested according to its joint benefits from heat mining and carbon sequestration (Singh et al., 2023). In a CO_2-EGS, CO_2 is injected into the HDR in its supercritical phase to extract heat after the construction of engineered fractures, such as hydraulic fracturing (Xue et al., 2023). Its large density and low viscosity make supercritical CO_2 (sCO_2) 2 ∼ 5 times more mobile than water (Song et al., 2019; Yang et al., 2023). In addition, sCO_2 can also be considered a potential large-scale electricity storage battery due to its extensive compressibility (Buscheck et al., 2016). Previous studies have proven the feasibility of a CO_2-EGS to provide a comparable heat mining performance in contrast to water-EGS (Tagliaferri et al., 2022; Liao et al., 2023). For example, Pruess (2006) indicated that, under the same amount of pressure drop, the CO_2-EGS can provide 4 times larger mass flows compared to the water-EGS, resulting in 50% larger heat mining rates. Furthermore, the extremely low solubility of minerals in sCO_2 can prevent scaling and corrosion problems in wellbore tubing and pipes.

CO_2 demonstrates certain advantages in the extraction of an EGS due to its higher mobility and injectivity (Sowiżdżał et al., 2022). However, its 40%–60% lower heat capacity than water on the mass basis makes CO_2-EGS require a greater mass outflux to extract the same amount of energy of a water-EGS (Zhang et al., 2014). On the other end, a higher mass flow rate means a higher resistance, which could degrade the heat mining performance of a CO_2-EGS. Importantly, the injected cold CO_2 is potentially considered a fast heat carrier in engineered high-conductive zones. As such, a temperature drop and a thermal breakthrough are unpreventably expected at an early stage, leading to a short project lifetime (Pruess, 2008; Shi et al., 2019a,b). Although these problems can be effectively resolved by decreasing the injection rate or pressure drop, the corresponding loss in the heat extraction rate could cause an insufficient geothermal energy recovery. Another significant challenge of CO_2-based geothermal operations is related to the geochemical reactions. The injected CO_2 is likely to trigger chemical reactions with the formation water and rock minerals (Xu et al., 2014, 2018). Although some portion of CO_2 can be fixed via geochemical mechanisms, the salt precipitation products can induce damage to the reservoir and degradation of heat mining rates (Isaka et al., 2019). Based on existing studies, the salinity of formation water shows a dominant effect on heat mining and CO_2 storage performance. Norouzi et al. (2021) implied that initial brine salinity is proportional to salt precipitation effects, and the heat extraction efficiency is inversely correlated to the salinity. On the other hand, Stefan (Iglauer, 2017) illustrated that CO_2 storage capacity is dramatically reduced with the brine salinity increases due to the enhanced CO_2-wettability. Therefore, it is recommended to utilize CO_2 in an EGS which is with tiny or no amount of formation water at the initial condition.

On the other hand, the geochemical reactions, such as salt precipitation still cannot be fully ignored in a CO_2-based EGS development (Esteves et al., 2019; Cui et al., 2019). To avoid salt precipitation in a geothermal reservoir under CO_2 utilization, pioneered investigations proposed a simultaneous injection scheme of CO_2 plus water in liquid-dominated geothermal reservoirs, such as CO_2-plume geothermal (CPG). Their results agreed that CO_2-water mixtures can effectively prevent salt precipitation because the dissolved CO_2 in water can minimize the water evaporation or salt precipitation (Zhang et al., 2016; Cui et al., 2016; Kaya et al., 2018). Meanwhile, several studies have also proven the heat transmission ability of CO_2-water mixtures. For example, Cui et al. (2018) revealed that a co-injection of CO_2 and water can improve the heat extraction rate of a CPG from 6 MW to 12 MW after 30 years of development compared to water. Salimi et al. (2012) also showed that an appropriate injected-CO_2 fraction can lead to up to 20% (1273 TJ) geothermal energy recovery. From the perspective of geologic CO_2 storage, the mixed working fluids of water and CO_2 also demonstrated some advantages, for example, the combined CO_2-water injection is possible to enhance residual trapping, and the leakage risk of CO_2 through the caprock can be effectively decelerated under dissolved CO_2 injection (Bryant et al., 2008). To the best of our knowledge, although the feasibility of co-injecting CO_2 and water has been established in a CPG system, there is no thorough systemic assessment framework on the applicability of CO_2-water-EGS in terms of heat mining and carbon sequestration. Besides, the techno-economic analysis incorporating the carbon policy for CO_2-water-EGS is necessary, which has not been well-established in pioneered studies. Importantly, there is no evidence to comprehend the determination of an optimal injection strategy for the operators.

In this research, we propose an integrated analysis from technical and economic perspectives based on the reservoir simulator (CMG-STARS) to investigate the feasibility of a CO_2-water-EGS involving the performance of heat mining associated with geologic carbon storage. The sensitivities of different operational parameters (i.e., the injection rate, injected CO_2 mass concentration, and flow scheme) are studied and an optimal operating scheme is determined. This study provides a comprehensive understanding of CO_2-water-EGSs at the system level by evaluating the technical and economic performance of heat mining and carbon storage, and hence practical guidance can be suggested for EGS operators in their decision-making processes.

2. Methodology

In this study, numerical and economic models are constructed to characterize the technical and economic feasibilities of the CO_2-water-EGS. The effects of three sensitive parameters (i.e., the injection rate, injected CO_2 mass concentration, and flow scheme) on heat extraction, carbon sequestration and economic performance are investigated. Meanwhile, the performance of water-EGS, CO_2-EGS and CO_2-water-EGS are comprehensively compared to determine their advantages and limitations from both the engineering and economic perspectives. In addition, different scenarios are developed in an optimization study to explore better operational strategies for CO_2-water-EGS development.

2.1. Reservoir model

The numerical models in this study are created by using CMG STARS software, which is a well-acceptable numerical simulator to solve a nonlinear system for multi-dimensional fluid flow analysis and heat transfers in multi-phase, multi-component fluids in porous and fractured media (Asai et al., 2019).

2.1.1. Mathematical model

The following reasonable assumptions are made to simplify the numerical models: (1) The chemical reactions in the reservoir are not considered; (2) The mechanical effects are not considered; (3) The aperture of the hydraulic fractures is assumed not to change during the heat extraction; (4) Local thermal equilibrium is applied, and there is no temperature difference between the fluid and rock in the same position.

The mathematical model mainly represents two physical processes, including fluid flow and heat transfer. The following two sets of conservative equations are solved by CMG STRARS: mass balance of fluid phase with Darcy's flux law and thermal energy balance. The CO_2-water mixture is considered as the working fluid in this study, which means it is a multi-phase and multi-component fluid flow in the model. Besides, water and CO_2 are also considered to develop the EGS separately in the sensitivity analysis (water-EGS: CO_2 mass ratio = 0; CO_2-EGS: CO_2 mass ratio = 1). The properties of water and CO_2 are calculated based on the CMG-Winprop module [39]. The mass conservation equation of the fluid flow in the porous media based on Darcy's law is written as Eq. (1) (Shi

et al., 2018):

$$\varphi\frac{\partial\rho_f}{\partial t}-\nabla\bullet\rho_f\left[\frac{k}{\mu_f}\nabla p+\rho_f g\nabla z\right]=-\rho_f S\frac{\partial p}{\partial t}-Q_f \tag{1}$$

Where φ is the reservoir porosity, ρ_f (kg/m^3) indicates the density of working fluid and t (s) is the time; k (m^2) is the reservoir permeability; μ_f (Pa • s) is the viscosity of the working fluid; p (Pa) denotes the pressure; $\rho_f g\nabla z$ represents the gravity term and z is the vertical direction; S (Pa^{-1}) is defined as the specific storage of the rock matrix; Q_f means the mass transfer between the rock matrix and fractures. Similarly, the fluid flow in the fractures is formulated by the mass conservation equation and Darcy's Law, which is calculated by Eq. (2) (Shi et al., 2019a,b):

$$d_f\varphi_f\frac{\partial\rho_f}{\partial t}-\nabla_T\bullet d_f\rho_f\left[\frac{k_f}{\mu_f}\left(\nabla_T p+\rho_f g\nabla z\right)\right]=-d_f\rho_f S_f\frac{\partial p}{\partial t}+d_f Q_f \tag{2}$$

Where d_f (m) is the fracture aperture and ∇_T represents the gradient operator restricted to the fracture's tangential plane; φ_f is the fracture porosity; k_f (m^2) and S_f (Pa^{-1}) represent the permeability and the specific storage of fracture respectively.

Thermal equilibrium transport is assumed between the solid and the fluid in this study, which has been validated to be an adequate method to predict the EGS performance. Therefore, the temperature of the solid and the working fluid are equal at any point in space and time. The heat transfer process in the porous media can be described by the energy conservation equation Eq. 3 (Shi et al., 2018):

$$\left(\rho C_p\right)_{eff}\frac{\partial T}{\partial t}+\rho_f C_{p,f}\boldsymbol{u}\bullet\nabla T-\nabla\left(\lambda_{eff}\nabla T\right)=-Q_{f,E} \tag{3}$$

Where T (K) is the temperature of the porous media; $C_{p,f}$ (J/(kg • K)) is the specific heat of the working fluid; $Q_{f,E}$ is the heat transfer between the porous media and fractures; $(\rho C_p)_{eff}$ represents the effective volumetric capacity and λ_{eff} (W/(m • K)) is the effective thermal conductivity, which can be expressed by volume averaging model to account for both reservoir rock and working fluid properties (Eqs. (4) and (5) respectively) (Shi et al., 2019a,b):

$$\left(\rho C_p\right)_{eff}=(1-\varphi)\rho_s C_{p,s}+\varphi\rho_f C_{p,f} \tag{4}$$

$$\lambda_{eff}=(1-\varphi)\lambda_s+\varphi\lambda_{eff} \tag{5}$$

Where ρ_s (kg/m^3) denotes the density of the solid part in the reservoir; $C_{p,s}$ (J/(kg • K)) is the specific heat of the solid and λ_s (W/(m • K)) represents the thermal conductivity of the solid part. Similarly, the energy conservation equation in fracture within the porous media can be expressed by Eq. (6) (Shi et al., 2018):

$$d_f\left(\rho C_p\right)_{eff}\frac{\partial T}{\partial t}+d_f\rho_f C_{p,f}\boldsymbol{u_f}\bullet\nabla_T T-\nabla_T\bullet\left(d_f\lambda_{eff}\nabla T\right)=d_f Q_{f,E} \tag{6}$$

Where the parameters $\boldsymbol{u}$ and $\boldsymbol{u_f}$ in the Eqs. (3) and (6) are the Darcy's velocity terms.

2.1.2. Numerical method

The base reservoir model is constructed based on our validated Qiabuqia EGS model in previous works (Xue et al., 2023a; 2023b; 2023c, 2024). Specifically, a dual permeability 2000 m (L) × 1000 m (W) × 3800 m (H) reservoir model with a total of 36,480 grid blocks is involved. Based on the explored geothermal gradient, the highest reservoir temperature of 236 °C was investigated at a depth of around 3700 m. Therefore, to extract geothermal power to the maximum extent, the underground area of 3,600 ~ 3700 m is determined as the study area with the consideration of the natural fractures according to the properties of this field (Lei et al., 2019; Zhang et al., 2019). The reservoir is assumed to be saturated with pure water at the initial condition to eliminate pore water to prevent salt precipitation (Cui et al., 2018). The key parameters in the base reservoir model are shown in Table 1. A detailed description of this field can be found in previous studies (Zhang et al., 2019; Lei et al., 2020). All boundaries of the reservoir are enclosed with no fluid flow. The heat loss model is used to govern heat losses from the top surface to the atmosphere at the top boundary. The initial temperature and pressure at the top of the study area are 236 °C and 37 MPa respectively.

Three horizontal wells, including an injection well (GR1) and two production wells (PR1 and PR2), are drilled at 3700 m underground with a well spacing of 500 m and a horizontal section length of 500 m. In terms of hydraulic fracture configuration, previous works have proven that the engineered fractures with a half-length from 250 to 670m, a height of 100m and a conductivity of 10mDm can be successfully constructed in Qiabuqia granite formation by injecting different amounts of slickwater (Lei et al., 2020). Thus, in this study, ten hydraulic fractures with a fracture spacing of 50 m are set to connect the production and injection wells with a half-length of 500 m, a height of 100m and a conductivity of 10mDm. The grids of fracturing area are refined five times in the horizontal directions and three times in the vertical directions aimed for an accurate calculation. The water and CO_2 mixture is utilized as the heat transmission fluid in this study. The 40 °C cold stream with a CO_2 mass ratio of 25%wt and a water ratio of 75%wt is injected into the reservoir. The injection rate is set to be 60 kg/s and the production pressure is assumed to be at 35 MPa. The heat mining and carbon storage performance are assessed after a twenty-year operating cycle. A schematic diagram of a three-horizontal-wells-based CO_2-water-EGS is shown in Fig. 1.

2.2. Investigated scenarios

In this study, the influences of the CO_2-water ratio, injection rate and flow scheme on heat extraction, carbon storage and economic performance are investigated. The CO_2 concentration is selected from 0%wt to 100%wt, and the injection rate is set from 30 kg/s to 90 kg/s. Besides, flow schemes are determined by variations in injection rates, which linearly increase or decline over time at a constant rate. The total amount of circulated working fluids is fixed among all scenarios. For example, in the 10-step-up scenario, the injection rate starts from 78 kg/s and gradually decreases by 4 kg/s every two years, and the injection rate at year 20 eventually reaches 42 kg/s. The 5-step-down case represents the injection rate declines every 4 years. On the contrary, the 5-step-up and 10-step-up cases mean the rate increases every 4 years and 2 years separately. The detailed information on scenario setting is shown in Table 2.

2.3. Computational indicators

To assess the technical and economic feasibilities of the CO_2-water-EGS, different indicators are determined. In specific, the installed

Table 1
Parameter setting of the base reservoir model.

Parameter	Value	Parameter	Value
Depth	3700	Granite specific heat, J/ (kg • °C)	980
Initial temperature, °C	236	Horizontal natural fracture spacing, m	10
Initial pressure, MPa	37	Vertical natural fracture spacing, m	10
Granite density, kg/m^3	2623	Injection rate, kg/s	60
Porosity, %	2.49	Injection temperature, °C	40
Horizontal permeability, mD	0.26	Mass CO_2 ratio of injected mixture, %wt	25
Vertical permeability, mD	0.026	Production pressure, MPa	35
Granite heat conductivity, W/ (m • °C)	3.0	Operation cycle, year	20

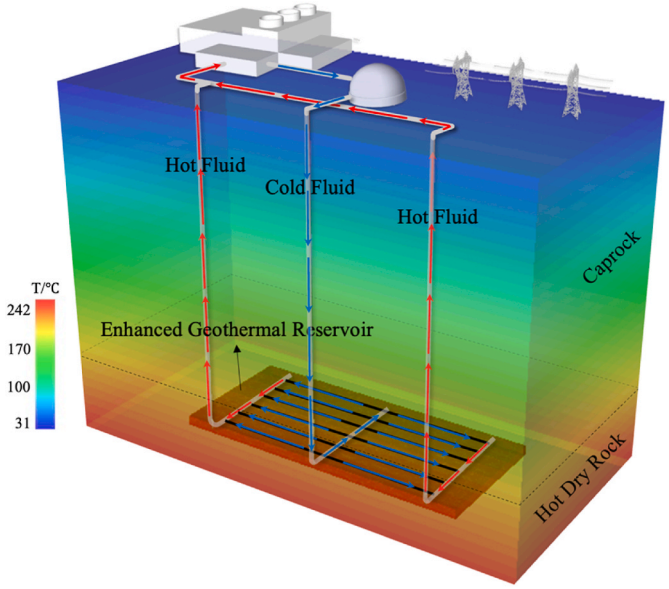

Fig. 1. Schematic diagram of a CO_2-water-EGS based on the numerical model.

geothermal electric power, CO_2 retention factor and cumulative stored CO_2 amount are calculated to study the engineering performance, and the net present value is estimated to determine the economic performance.

2.3.1. Technical indicators

The calculation measures are established from both the heat mining and carbon storage perspectives. Specifically, the generated geothermal electricity (E) is used to quantify the heat mining recovery (Eq. (7)). The CO_2 retention factor (R_{CO_2}) and cumulative stored CO_2 amount ($M_{stored\_CO_2}$) are considered to evaluate the carbon sequestration performance because these two factors are commonly used during the field operation (Azzolina et al., 2015; Ma et al., 2022), which are expressed by Eqs. (8) and (9) (Ma et al., 2022a, 2022b; Yu et al., 2022), separately.

$$E = \sum_{t}^{T} W_p^t \bullet H_{annual} \bullet 0.9 \tag{7}$$

$$\text{where: } \begin{cases} W_p = 0.45 \bullet Q \bullet \Delta H \bullet (1 - T_{rej}/T_{out}) \\ H_{annual} = 365 \bullet 24 \end{cases}.$$

$$R_{CO_2} = \left(M_{CO_2,inj} - M_{CO_2,prod}\right) / M_{CO_2,inj} \tag{8}$$

$$M_{stored\_CO_2} = M_{CO_2,inj} - M_{CO_2,prod} \tag{9}$$

Where W_p^j (W) indicates the annual geothermal power capacity; the capacity factor is assumed as 0.9; Q (kg/s) is a fluid production rate in the whole system, ΔH (J/kg) is an enthalpy change between the injected enthalpy and produced enthalpy; T_{rej} (K) is the rejection temperature; T_{out} (K) is the average temperature of the production wells; $M_{CO_2,inj}$ (kg) and $M_{CO_2,prod}$ (kg) represent the total injected and produced CO_2 respectively; T is the number of operation time periods.

2.3.2. Economic indicator

In addition to technical indicators for reservoir performance, the net present value (NPV) is utilized to estimate the economic reaction by Eq. (10), which contains the capital expenditure (CAPEX), operating expenditure (OPEX), obtained geothermal energy revenue, earned carbon credit and revenue tax.

$$NPV = -CAPEX + \sum_{t-1}^{T} \left(R_{energy\_revenue} + R_{credit} - OPEX - C_{tax}\right) / (1 + r_d)^t \tag{10}$$

Table 2
Parameter setting of various scenarios.

Investigated parameter	Scenario	CO_2-water mass ratio	Injection rate	Flow scheme
CO_2-water ratio	#1	0% CO_2 + 100% water	60 kg/s	constant
	#2	25% CO_2 + 75% water	60 kg/s	constant
	#3	50% CO_2 + 50% water	60 kg/s	constant
	#4	75% CO_2 + 25% water	60 kg/s	constant
	#5	100% CO_2 + 0% water	60 kg/s	constant
Injection rate	#6	25% CO_2 + 75% water	30 kg/s	constant
	#7	25% CO_2 + 75% water	45 kg/s	constant
	#8	25% CO_2 + 75% water	60 kg/s	constant
	#9	25% CO_2 + 75% water	75 kg/s	constant
	#10	25% CO_2 + 75% water	100 kg/s	constant
Flow scheme	#11	25% CO_2 + 75% water	/	10 steps down
	#12	25% CO_2 + 75% water	/	5 steps down
	#13	25% CO_2 + 75% water	60 kg/s	constant
	#14	25% CO_2 + 75% water	/	5 steps up
	#15	25% CO_2 + 75% water	/	10 steps up
Notes:	10 steps down:	Initial rate: 78 kg/s;	Growth: 4 kg/s (every 2 year);	Finial rate: 42 kg/s
	5 steps down:	Initial rate: 70 kg/s;	Growth: 5 kg/s (every 4 year);	Finial rate: 50 kg/s
	Constant:	Initial rate: 60 kg/s;	Growth: 0 kg/s;	Finial rate: 60 kg/s
	5 steps up:	Initial rate: 50 kg/s;	Growth: +5 kg/s (every 4 year);	Final rate: 70 kg/s
	10 steps up:	Initial rate: 42 kg/s;	Growth: +4 kg/s (every 2 year);	Final rate: 78 kg/s

$$\textit{where: } \begin{cases} CAPEX = C_{surface} + C_{drilling} + C_{stimulation} \\ *C_{surface} = 2000 \bullet exp\,(-0.045 \bullet (\dot{W}_p - 5)) \\ *C_{drilling} = 600 \bullet H_v + 1500 \bullet H_h \\ *C_{stimulation} = 0.3 \bullet C_{drilling} \\ OPEX = C_{O\&M} + C_{fluid\_purchase} \\ *C_{O\&M} = 20 \bullet \exp(-0.0025 \bullet (\dot{W}_p - 5)) \\ R_{energy\_revenue} = E \bullet P_{electricity} \\ R_{credit} = Q_{CO_2} \bullet P_{CO_2} \\ C_{tax} = 0.15 \bullet C_{revenue} \end{cases}.$$

Where CAPEX includes the investments of surface facilities ($C_{surface}$) and drilling ($C_{drilling}$) and reservoir stimulation ($C_{stimulation}$) and OPEX includes the operation and maintenance costs ($C_{O\&M}$) and fluid purchase costs ($C_{fluid\_purchase}$). In CAPEX, $C_{surface}$ of a geothermal project is the functions of geothermal power capacity according to previous works (Chamorro et al., 2012); The drilling expenses of a vertical well and a horizontal well are assumed as $600/m and $1500/m respectively (Lei et al., 2020); The investment in reservoir stimulation is estimated to be 30% of the drilling cost (Xie and Wang, 2022). In OPEX, $C_{O\&M}$ can also

be calculated based on geothermal power capacity (Chamorro et al., 2012); The unit purchase costs of CO_2 and water are set to be \$30/ton and \$0.66/ton based on the published data on fluid price for related projects (Jiang et al., 2019). For the energy revenue, the electricity retail price ($P_{electricity}$) is set to be 0.09\$/kWh according to the reported data on electricity selling price (Xu et al., 2022). Besides, the stored CO_2 in the industry or power generation can receive tax credit according to IRC 45Q, which is assumed as \$45/ton in this study, where Q_{CO_2} is cumulatively stored CO_2 and P_{CO_2} indicates the carbon price for geological sequestrated CO_2. In addition, 15 % of the obtained revenue from EGS development is determined as the total related tax and royalty payments in this work, and a 10% annual discount rate (r_d) is used to discount the future cash flow into the present monetary value. The detailed parameter setting of the NPV model is shown in Table 3.

2.4. Optimization study

To determine the optimal working strategy, an optimization study is conducted by using the CMG-CMOST module. Based on the created base reservoir model, CMG-CMOST conducts a random selection of different investigated parameters and then creates corresponding models. Each operational configuration is adopted into a separate model and the results are further calculated. In this study, the objective is to maximize the NPV function (Eq. (10)) by finding the optimal combination of two operational factors, injection rate and CO_2-water ratio, which are also defined as the decision variables. The operational constraints are that the injection pressure should be lower than the minimum principal stress to prevent slippage from occurring and a much lower injection rate is not desirable since it cannot support promising geothermal energy recovery. Based on our investigation, the injection pressure increases with the injection rate increases and the CO_2 mass ratio decreases. When the CO_2 mass ratio is assumed as 0%wt, the injection pressure would be higher than the minimum principal stress if the injection rate exceeds 110 kg/s. Therefore, the injection rate is stochastically selected in a range from 20 kg/s to 110 kg/s. The CO_2 ratio represents the concentration of CO_2 in the working fluid in the mass basis wt%. For example, a 0.2 CO_2 ratio means that the CO_2 mass concentration of injected fluid is 20%wt and the rest 80%wt is water. The range of CO_2 ratio is set to be from 0%wt to 100%wt in this work. In total, 625 simulations are performed associated with the corresponding technical and economic indicators. The optimal strategies can be therefore determined by conducting the scenario-based analysis.

3. Results

In the results of this study, the effect of the CO_2-water mass ratio in the injection fluid is introduced, and the technical and economic performance of CO_2-water-EGS is compared with water-EGS and CO_2-EGS. In addition, the results of the scenarios with various injection rates and different flow schemes are demonstrated to explore their influences. Consequently, the optimization result is illustrated to determine the optimal operational strategy for the CO_2-water-EGS and to explore the combined influence of the CO_2-water ratio and injection rate on heat mining, carbon storage and economic performance.

Table 3
Parameter setting of the NPV model.

Parameter	Value
Drilling cost of a vertical well (\$/m)	600
Drilling cost of a horizontal well (\$/m)	1500
Electricity retail price (\$/kWh)	0.09
Water purchase cost (\$/ton)	0.66
CO_2 purchase cost (\$/ton)	30
Carbon credit rate (\$/ton)	45
Tax rate (%)	15

3.1. Model validation

The field development of the Qiabuqia geothermal field has not started and thus the real production data is not available currently. Therefore, the numerical model in this study is validated by comparing its results with that of Lei's model which is a well-accepted Qiabuqia EGS model. By setting the parameters of our model to be the same as those of Lei's model, the results of production temperature and generated geothermal power are compared, which is shown in Figs. 2 and 3 respectively. From the results, the production temperature and geothermal electricity between our model and their model are highly consistent, where two stages (a stable stage and a declining stage) are shown in both the production temperature and geothermal electricity during an operating cycle, and the errors are all only about 2%. The main reason for these errors is the differences in fracture properties setting. In Lei et al.'s model, an average permeability of 100 mD was substituted for the five hydraulic fractures, which was computed by the permeability of the original granite and the hydraulic fractures. In our model, five fractures are generated with the original reservoir permeability unchanged, which can more accurately represent an underground stimulated reservoir. Therefore, our model is reasonable for predicting the development of the Qiabuqia geothermal field.

3.2. Effects of CO_2-water ratio

In this section, the effects of the CO_2-water ratio on heat extraction, carbon sequestration and economic performance are investigated (scenarios #1 ~#5 in Table 2). Figs. 4 and 5 demonstrate the average production temperature, installed geothermal power and generated electricity under different CO_2-water ratios. From Fig. 4, a larger temperature drop is observed in the scenario with a higher CO_2 mass concentration in the working fluid. This is because the circulating fluid flows at a larger speed in the reservoir when more CO_2 is injected and the cold injection fluid connects to the production sides earlier. Therefore, a larger CO_2 mass ratio in the injection fluid shows a shorter project lifetime. Differently, the extracted geothermal electricity is not monotonically changed with the CO_2-water ratio (Fig. 5), which is increased with the CO_2 concentration from 0%wt to 25%wt and then decreased with the CO_2 ratio from 25%wt to 100%wt. In these cases, the scenario of 25%wt CO_2 contributes the highest geothermal electricity (1520.55 GWh), while the lowest (1041.80 GWh) can be observed in the case when injecting 100%wt CO_2 (pure CO_2-EGS). Although the cases with lower CO_2 mass ratio can provide higher production temperatures, their lower flow rates induce less hot working fluid being produced so that the

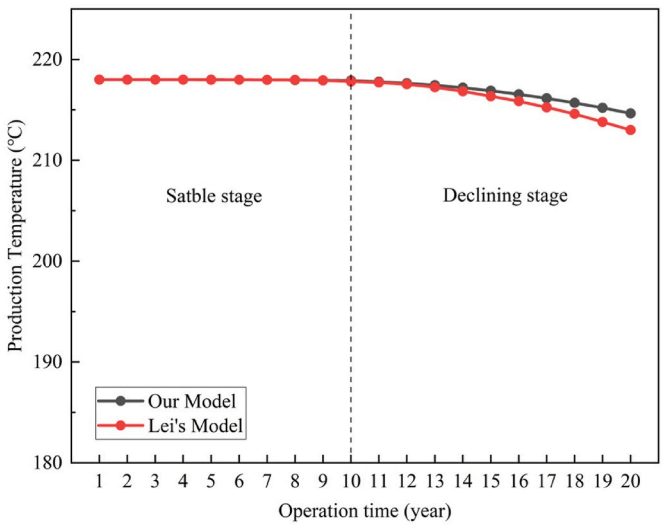

Fig. 2. Model validation based on the production temperature.

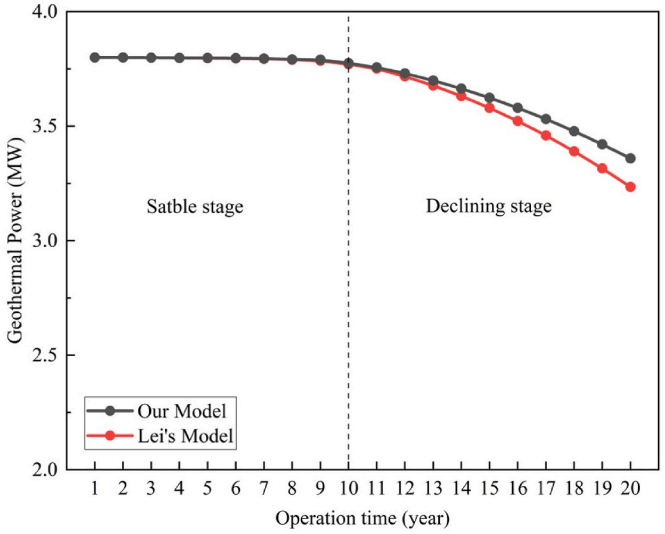

Fig. 3. Model validation based on the geothermal power generation.

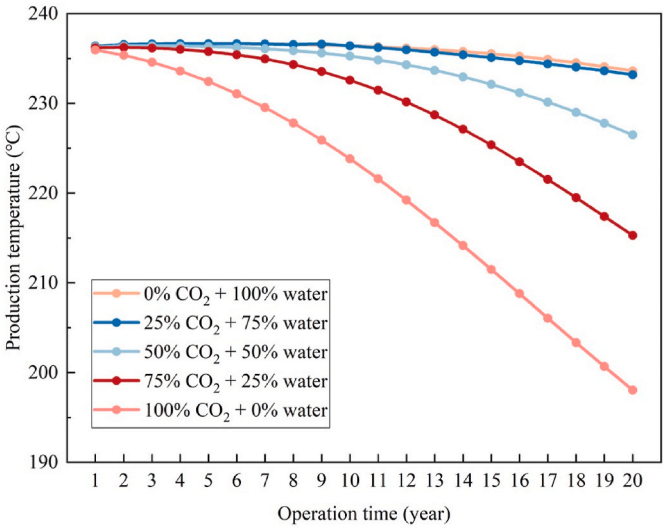

Fig. 4. Production temperature under various CO_2-water ratios.

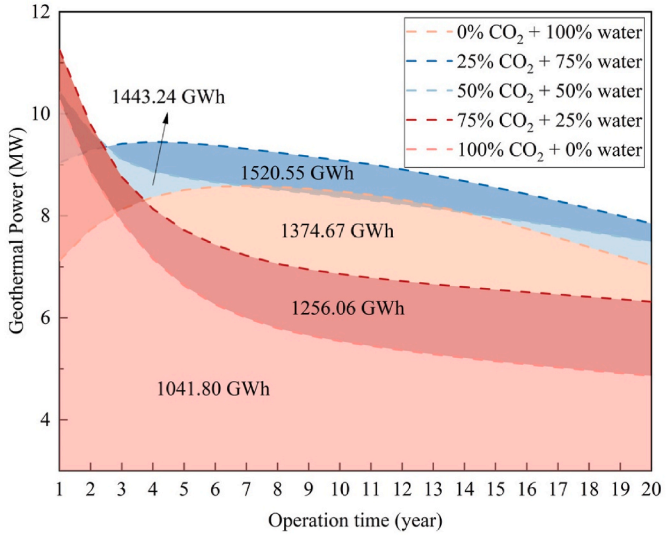

Fig. 5. Geothermal power and electricity generation under various CO_2-water ratios.

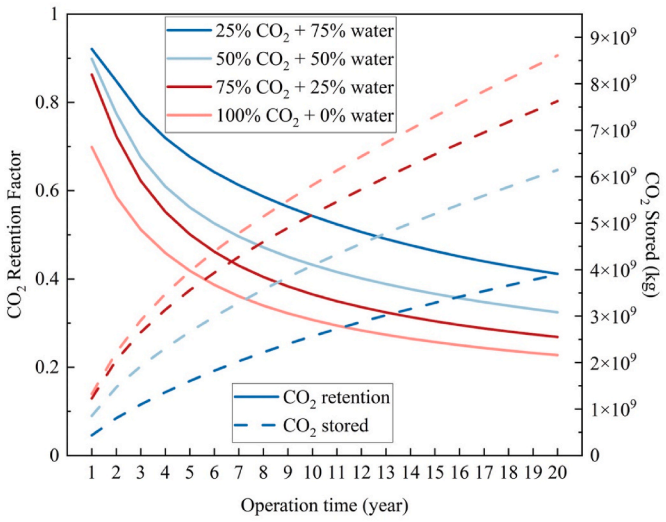

Fig. 6. CO_2 retention factor and cumulative stored CO_2 under various CO_2-water ratios.

generated geothermal energy is lower. With the increment of CO_2 mass concentration, the resulting higher production rate contributes to more produced geothermal energy. However, if the production rate exceeds a certain value, the temperature drop and thermal breakthrough are more likely to occur at an early stage, resulting in the temperature of the produced fluid not stabilizing at a high level and not promising extracted geothermal energy. This can also explain the results that a higher CO_2 concentration tends to induce a more dramatic decrease in geothermal power based on their profiles. Fig. 6 shows the effects of the CO_2-water ratio on the CO_2 retention factor and cumulative stored amount of CO_2, and the results illustrate that a larger amount of CO_2 can be stored in the reservoir under a higher concentration of CO_2 while the relationship between the CO_2 retention factor and CO_2 concentration presents a reverse trend. Although increased CO_2 concentration can provide a demonstrable growth in CO_2 storage capacity, its lower CO_2 retention factor validates that a higher CO_2 ratio in the working fluid is unavoidable to induce a faster breakthrough time.

To determine the economic performance, the NPV profiles and detailed economic results are presented in Fig. 7 and Table S1 respectively. In all the NPV curves, the negative initial NPV is observed due to the capital-intensive of an EGS project. The initial NPV is influenced by the heat mining performance since a larger geothermal energy generation requires a higher investment in CAPEX, explaining that the 25%wt CO_2 shows the lowest initial NPV while the 100%wt CO_2 is the highest. With the profits from retailing geothermal electricity and earning carbon credit, the NPV increases gradually. However, the 100%wt CO_2 shows a different trend, where its NPV starts to grow in the second year. This is because its huge CO_2 consumption makes its income cannot cover the cost of CO_2 consumption before this period. Accordingly, it is hard to pay back until the eighth year. In the 25%wt CO_2 and 50%wt CO_2, faster increase trends in NPV are investigated due to their higher geothermal electricity generation and less CO_2 consumption, resulting in paybacks in the 4th year and the NPV of 31.5 M$ and 31.8 M$ respectively. Compared to 50%wt CO_2, the 25%wt CO_2 shows a higher growth rate in NPV at the beginning of the operation but then illustrates a lower growth rate. This is because the 25%wt CO_2 demonstrates a stable trend in power generation while the 50%wt CO_2 illustrates a dramatic decline trend at the beginning, but with the development, the power production of the 25%wt CO_2 shows a larger decline speed than that of the 50%wt CO_2 (Fig. 3). In the 75%wt CO_2, a payback period of 5 years is obtained

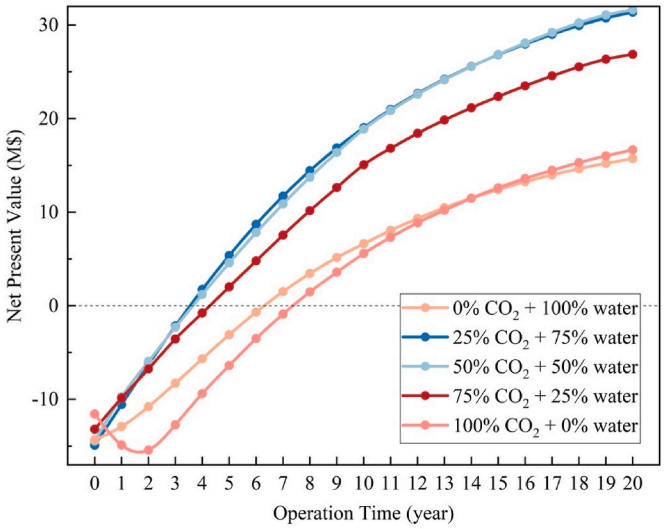

Fig. 7. Net present value under various CO_2-water ratios.

because of more investment in purchasing CO_2 and lower geothermal electricity generation compared to the 25%wt CO_2 and 50%wt CO_2, and a final NPV of 26.9 M$ is obtained. It should be also noted that the case of 0%wt CO_2 (water-EGS) demonstrates a higher NPV than the case of 100%wt CO_2 (CO_2-EGS) in the early period due to its lower cost in fluid purchasing, but without a tax credit from carbon sequestration, its NPV in the 20th year is lower than for CO_2-EGS. Although the case of 100%wt CO_2 can build the highest CO_2 tax credit, its largest investment in fluid consumption makes it not promising in economic benefits.

3.3. Effects of injection rate

In this section, the effects of injection rate on production temperature, heat extraction and carbon sequestration performance are shown in Figs. 8–10 respectively (scenarios #6 ~#10 in Table 2). Based on Fig. 8, a higher injection rate accounts for a lower production temperature since the resulting higher flow rate makes the cold fluid flow to the production wells faster and more temperature drop can be observed. Therefore, the project lifetime decreases with the increment of injection rate. It also explains better heat mining performance is obtained in higher injection rate cases (Fig. 9). To be specific, the 90 kg/s injection

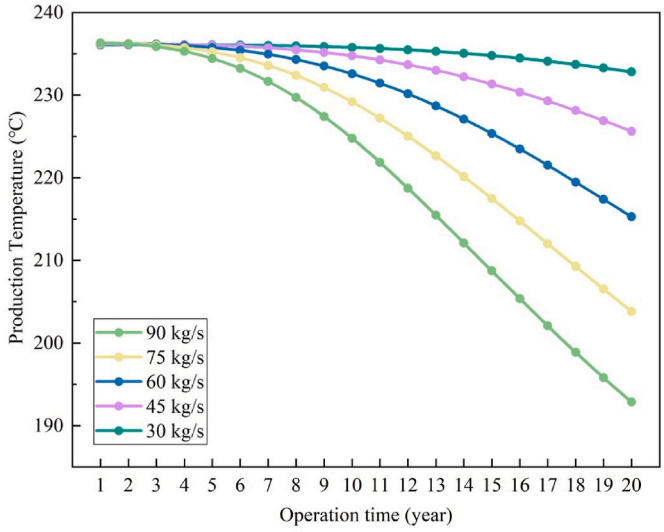

Fig. 8. Production temperature under various injection rates.

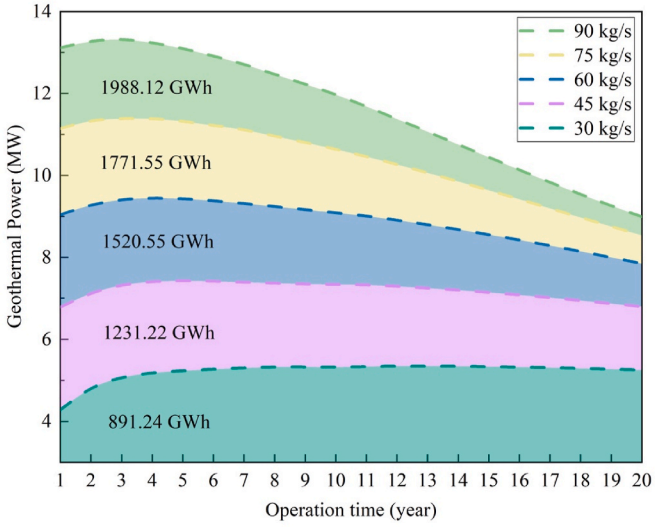

Fig. 9. Geothermal power and electricity generation under various injection rates.

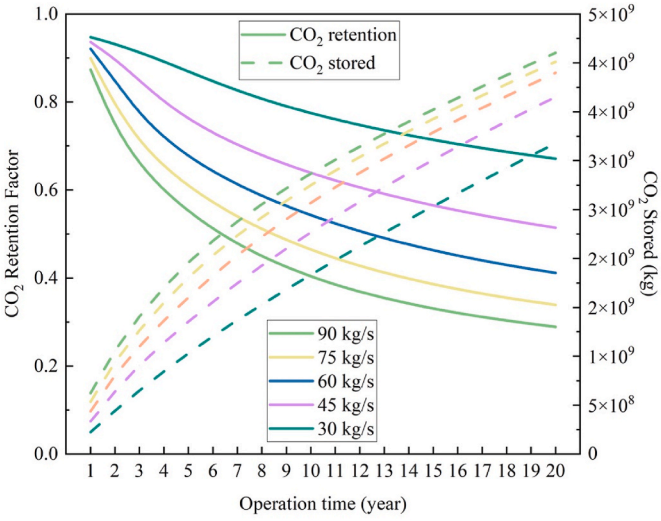

Fig. 10. CO_2 retention factor and cumulative stored CO_2 under various injection rates.

rate results in the highest geothermal electricity generation of 1988.12 GWh, while the 30 kg/s injection rate leads to the lowest electricity production (891.24 GWh). Under consistent production pressure, the heat production rate is proportional to the injection rate. As such, the 90 kg/s injection rate starts with the highest installed geothermal power in the first year (13.1 MW) but that in the 30 kg/s is the lowest (4.3 MW). However, the highest production rate in the scenario with a 90 kg/s injection rate triggers the fastest temperature drop and thermal breakthrough in the time horizon, and thus, the largest decline in generated geothermal power is demonstrated. On the contrary, the 30 kg/s injection rate shows a more stable production profile. Fig. 10 illustrates that a faster injection rate can bring a larger amount of cumulative stored CO_2 but a smaller CO_2 retention factor, which also validates the breakthrough is probably provoked at an earlier stage when the CO_2 is injected into the reservoir at a higher rate.

The economic performance of the EGSs under various injection rates is presented in Fig. 11 and Table S2. As illustrated, the NPV of all the scenarios presents a gradually increasing trend. Due to the highest geothermal energy production, the largest CAPEX is required for the 90 kg/s injection rate and therefore the lowest NPV is observed in its initial

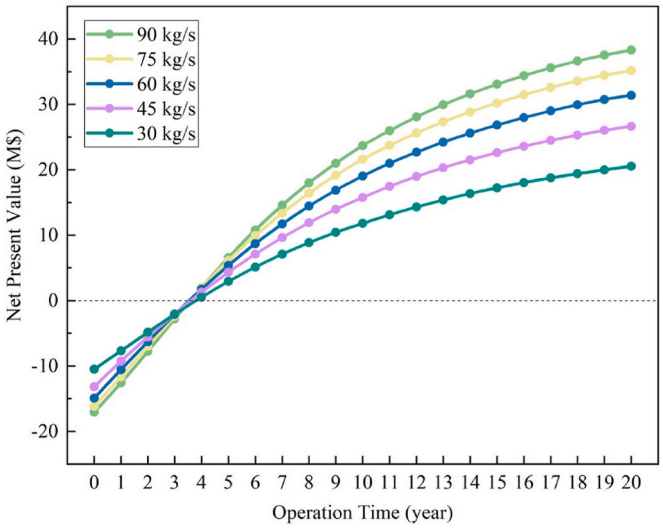

Fig. 11. Net present value under various injection rates.

state. Reversely, the highest initial NPV is observed in the 30 kg/s injection rate. Subsequently, with a higher annual income from retailed geothermal electricity and received carbon credit, the cases with a larger injection rate present a faster growth rate in the NPV, which causes the same payback period of 4 years can be detected in these cases. Finally, the 90 kg/s injection rate shows the highest NPV of 38.3 M$ at the end of 20-year operation but the 30 kg/s injection rate demonstrates the lowest NPV of 20.5 M$. In short, a larger injection rate is preferred in developing an EGS because the injection rate shows positive relationships to heat extraction, carbon storage and economic performance. However, generated geothermal energy at a higher injection rate is hard to stabilize at a promising level during the long-term EGS operation. Therefore, a small injection rate is recommended for the operators driven by long-term EGS power generation but a high injection rate can be utilized if the project tends to extract the geothermal energy as much as possible at a certain operation time.

3.4. Effects of flow scheme

In this section, different flow schemes are carried out to investigate their influence on production temperature, heat mining, carbon storage and economic performance (scenarios #11 ~#15 in Table 2). Fig. 12 illustrates that various flow schemes show similar production temperatures at the end of a 20-year operation when the same total amount of circulated working fluids is utilized. The production temperatures in the cases of 10 and 5 step-up show slow decreases at an early stage due to their lower initial injection rates but then decline faster with the increment of injection rate, while those in the cases of 10 and 5 step-down demonstrate the opposite phenomenon. Therefore, in Fig. 13, the highest initial injection rate makes the 10-step-down with the highest geothermal power generation in the first year (11.5 MW) but a dramatic decline in power production is observed due to its gradually decreased injection rate until around 6 MW is obtained in the 20th year. Similarly, the geothermal power generation of the 5-step-down decreases from 10.5 MW to 6.8 MW. Reversely, with a steady enhancement in injection rate, the 5-step-up and 10-step-up all provide a moderately increasing production profile, where the installed power enhances from 7.5 MW to 8.9 MW in the 5-step-up and from 6.2 MW to 9.7 MW in the 10-step-up. Although all the scenarios present different heat mining performances during a 20-year operation, the highest cumulative geothermal electricity generation of 1544.23 GWh is found in the 10-step-down and the lowest is 1498.07 GWh in the 10-step-up, which is only around a 3% variance, indicating little effect of flow schemes on heat extraction consequences.

Fig. 14 shows the performance of carbon sequestration. Fig. 15 and Table S3 present the economic consequences of various flow schemes. As mentioned in the previous section, the stored amount of CO_2 is increased with the injection rate. Therefore, from Fig. 14, the sequestrated CO_2 of 10-step-down is higher than other cases at the early stage and then shows a decreased increment until lower than other cases after the 14th year. However, during a 20-year operation, all the scenarios demonstrate similar results in CO_2 retention factor and cumulative stored amount of CO_2. Therefore, it can be concluded that the flow scheme has little influence on carbon sequestration performance. In terms of economic performance, results validate that the profits obtained from various scenarios are similar (Fig. 12). Specifically, benefiting from higher generated geothermal electricity and CO_2 storage amount, the 10-step-down and 5-step-down bring a faster increasing NPV in the initial phase among all the cases. Whereas, a smaller NPV growth rate can be investigated then due to gradually decreased geothermal energy recovery and CO_2 sequestration capacity. In contrast, the 5-step-up and 10-step-up cases can provide a more stable growth rate in their NPV curves because of their steadily increased revenue from heat mining and carbon storage. Consequently, it can be concluded that various flow

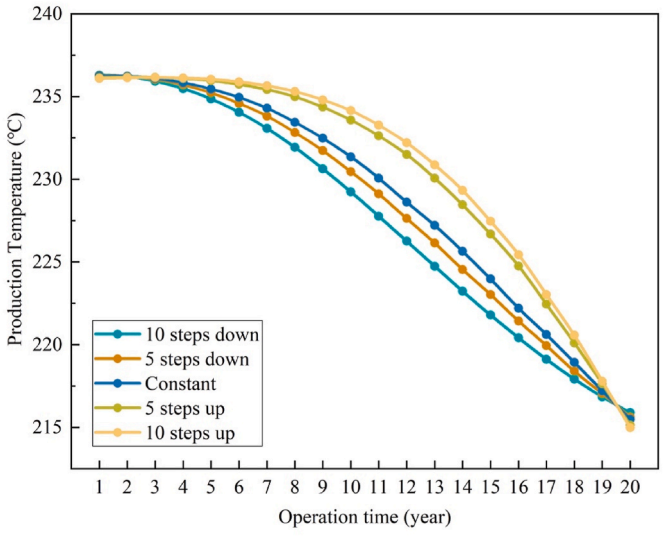

Fig. 12. Production temperature under various flow schemes.

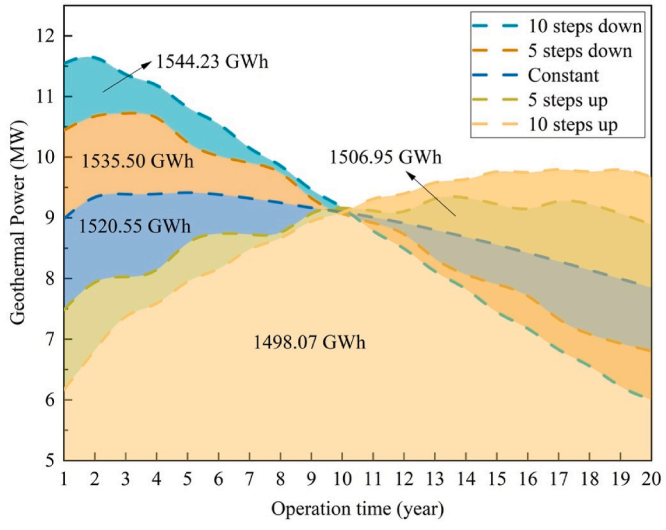

Fig. 13. Geothermal power and electricity generation under various flow schemes.

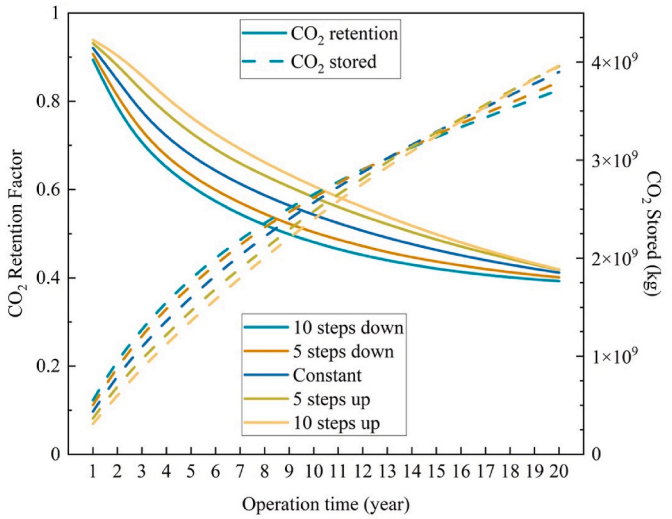

Fig. 14. CO_2 retention factor and cumulative stored CO_2 under various flow schemes.

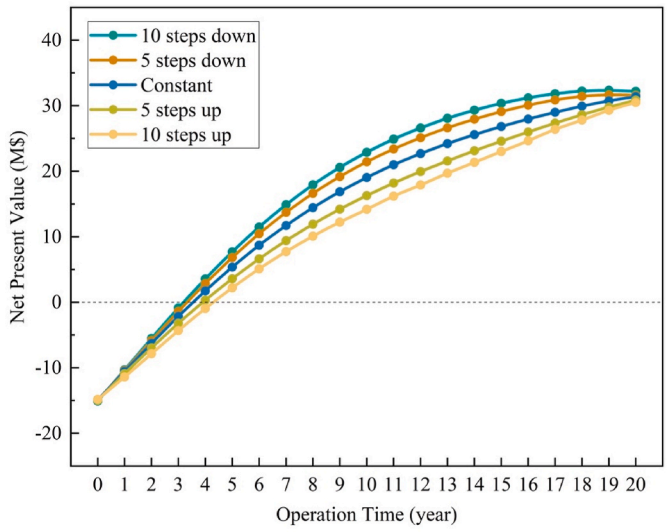

Fig. 15. Net present value under various flow schemes.

schemes show little effect on heat extraction performance, carbon sequestered volume and NPV when the cumulative amount of injection fluid is consistent.

3.5. Optimized injection strategy

In this section, the optimal configuration of injection rate and injected CO_2 mass ratio contributing to the highest NPV is presented, which is shown in Fig. 16. From the results, the case that received the highest NPV is under a 110 kg/s injection rate and a 20%wt CO_2 mass concentration in the injection fluid, where the project can earn 42.4 M$ after a 20-year operation. Comparatively, the CO_2-EGS (100%wt CO_2) under a 110 kg/s injection rate shows the lowest NPV of 1.2 M$ due to its huge investments in purchasing CO_2. Meanwhile, the water-EGS (0% wt CO_2) under a 20 kg/s injection rate also performs not promising in economics due to its undesirable heat mining performance and zero carbon storage amount. However, due to no investment in purchasing expensive CO_2, its NPV reaches 5 M$. In addition, it can be concluded that the strategy of a lower injection rate and a lower CO_2 ratio and the scheme with a higher injection rate and a higher CO_2 ratio are not

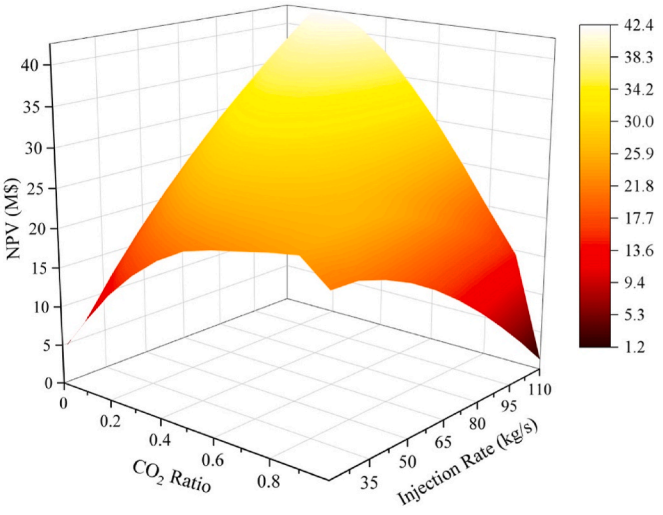

Fig. 16. Optimization results based on economic performance.

recommended in developing an EGS due to their unsatisfactory NPV results. In contrast, the case with a higher injection rate with a lower CO_2 ratio or the strategy of a lower injection rate with a higher CO_2 ratio performs better in economics, which can provide the operators with a valuable suggestion for developing different EGSs. Considering the field constraint that the injection pressure should be lower than the minimum principle stress, the injection rate should be customized for various EGSs due to their different geological properties. Therefore, as the injection rate is selected, the operators can further determine the injected CO_2 mass concentration based on the results of this study.

4. Discussion

Water-EGS and CO_2-EGS have been widely investigated in pioneer studies, and their results have validated that these two conventional EGS operations demonstrate some limitations from technical and economic perspectives. Specifically, water-EGS illustrates the disability in reducing additional carbon emissions and earning more profits by achieving subsurface carbon storage. Due to the low heat capacity of CO_2, CO_2-EGS shows the problem of an early thermal breakthrough when a large production rate is achieved for desirable heat mining performance. This study proposes a novel CO_2-water-EGS and analyzes its technical and economic feasibility. The results indicate that by selecting the appropriate CO_2-water ratio of injection fluid, CO_2-water-EGS can end up with a higher geothermal energy extraction than water-EGS and CO_2-EGS. Meanwhile, the economic performance of CO_2-water-EGS outperforms either water-EGS or CO_2-EGS. Although CO_2-EGS shows the best carbon storage performance, its earliest thermal breakthrough and significant amount of CO_2 consumption drive insufficient power generation and expensive monetary expense on CO_2 purchase. Therefore, the proposed CO_2-water-EGS can simultaneously unlock the disability of water-EGS in storing CO_2 in the reservoir and mitigate the question of an early thermal breakthrough in CO_2-EGS, but an optimal CO_2-water ratio should be investigated in different EGS projects.

The application of CO_2-water mixtures in heat extraction has been studied but it was only studied in the CPG. For example, Salimi et al. (2012) selected three injected CO_2 mole fractions (2%, 3% and 7%) to explore the heat mining and carbon storage performance of a CPG. Zhao et al. (2023) studied the heat extraction rate of a CPG under the CO_2 mass fraction of 32% ~ 85%. Cui et al. (2018) considered one CO_2-water ratio to study the production rate of a CPG. Although the feasibility of CO_2-water mixtures in heat mining or carbon storage can be validated by several selected CO_2 fractions, the influence of CO_2 concentration on reservoir performance is incomprehensive. For instance, the results in

Zhao's study indicated that the heat transfer effect is decreased with the CO_2 concentration increased from 32% ~ 85% (Zhao et al., 2023). However, the effect of the CO_2 ratio beyond this range was not investigated. Instead, a CO_2 mass fraction from 0%wt to 100%wt is selected in our study and the results illustrate that heat mining performance is not monotonically changed with the CO_2 mass fraction in this range. Importantly, an EGS highly differs from a CPG in technical and economic performance. This study fills the gap in the application of CO_2-water mixture in EGSs. The comparison among CO_2-water-EGS, Water-EGS and CO_2-EGS provides solid evidence of the advantages of utilizing CO_2-water mixtures as a heat transmission fluid.

Given the profitability as the major obstacle for current EGS development, a practical suggestion of the optimal CO_2-water ratio and injection rate selections contributing to the maximum profit for the operators in utilizing mixed CO_2-water fluid is still ambiguous according to previous studies. In this study, an optimization study with the consideration of various configurations of injection rate and CO_2 mass ratio is conducted, and the results present that the schemes with an injection rate of 110 kg/s and a CO_2 concentration of 20%wt can bring the largest profit. The optimization results also provide valuable insight for the operators in determining the injection strategy when developing other EGS projects, where the injected CO_2 mass ratio is recommended to be lower if a higher injection rate has been determined. Based on current technology and policy, the expensive CO_2 purchasing price is the major obstacle for an EGS under CO_2 utilization. With the possible decreased CO_2 purchasing price due to the technology improvement and the potential increment in carbon tax credit according to IRC 45Q, the operators can then consider a higher injection rate and a higher CO_2 concentration for an EGS project. Although this study provides a comprehensive insight into the subsurface performance of an EGS operation, it could be further improved by investigating the impact of different reservoir properties on the technical and economical performance of the CO_2-water-EGS.

5. Conclusions

In this study, the technical and economic feasibilities of a CO_2-water-EGS are investigated. The effects of injection rate, CO_2-water ratio and flow scheme are comprehensively analyzed from heat mining, carbon storage and economics perspectives. Followed by an optimization process based on 625 scenarios to determine the optimal injecting strategy. This study provides a comprehensive insight into the subsurface performance of an EGS operation and an informative decision-making strategy for both operators and investors in determining the appropriate operational schemes. The main findings of this work can be summarized as follows:

(1) The CO_2-water-EGS under a 25%wt CO_2 mass ratio in the injection fluid demonstrates the best heat mining performance. In contrast, the heat mining performance of the water-EGS (0%wt injected CO_2 ratio) is lower because of its lower production rate, and that of the CO_2-EGS (100%wt injected CO_2 ratio) is the lowest due to the earliest thermal breakthrough.
(2) Benefiting from the higher heat extraction rate, a higher injection rate contributes to higher geothermal energy generation but causes an earlier thermal breakthrough and further reduces the lifetime of the project. When a consistent total amount of working fluid is utilized, different flow schemes with variant injection rates show little influence on heat extraction performance.
(3) In the performance of carbon sequestration, more CO_2 can be stored in the reservoir when more amount of CO_2 is injected. Therefore, a higher CO_2 mass concentration or a higher injection rate contributes a larger amount of CO_2 subsurface storage and the scenarios with the consistent total amount of working fluid show similar carbon storage performance.
(4) The case with a 25%wt injected CO_2 mass ratio shows the highest NPV due to the best heat mining performance. Although CO_2-EGS obtains the highest carbon credit, its worst heat mining performance and largest CO_2 consumption induce an undesirable NPV. A higher injection rate can bring a larger NPV owing to its better heat mining and carbon storage performance.
(5) In the optimization study, an optimal scenario is determined as the configuration of 110 kg/s and 20%wt CO_2 and can bring the highest NPV of 42.4 M$. To earn more profits, it is suggested that a lower injected CO_2 mass concentration should be considered when a larger injection rate has been determined or a larger injected CO_2 mass ratio should be selected in case of a lower injection rate.

CRediT authorship contribution statement

Zhenqian Xue: Writing – review & editing, Writing – original draft, Validation, Software, Methodology, Investigation, Formal analysis, Data curation, Conceptualization. **Haoming Ma:** Writing – review & editing, Visualization, Resources, Methodology. **Zhe Sun:** Writing – review & editing, Resources. **Chengang Lu:** Writing – review & editing, Resources. **Zhangxin Chen:** Writing – review & editing, Supervision, Resources, Methodology, Investigation.

Declaration of competing interest

The authors declare that they have no known competing financial interests or personal relationships that could have appeared to influence the work reported in this paper.

Data availability

Data will be made available on request.

Acknowledgments

This research has been made possible by contributions from the Natural Sciences and Engineering Research Council (NSERC)/Energi Simulation Industrial Research Chair in Reservoir Simulation, the Alberta Innovates (iCore) Chair in Reservoir Modeling, and the Energi Simulation/Frank and Sarah Meyer Collaboration Centre.

Appendix A. Supplementary data

Supplementary data to this article can be found online at https://doi.org/10.1016/j.jclepro.2024.141749.

References

Aghahosseini, A., Breyer, C., 2020. From hot rock to useful energy: a global estimate of enhanced geothermal systems potential. Appl. Energy 279, 115769. https://doi.org/10.1016/j.apenergy.2020.115769.
Anderson, A., Rezaie, B., 2019. Geothermal technology: trends and potential role in a sustainable future. Appl. Energy 248, 18–34. https://doi.org/10.1016/j.apenergy.2019.04.102.
Asai, P., Panja, P., McLennan, J., Moore, J., 2019. Efficient workflow for simulation of multifractured enhanced geothermal systems (EGS). Renew. Energy 131, 763–777. https://doi.org/10.1016/j.renene.2018.07.074.
Azzolina, N.A., Nakles, D.V., Gorecki, C.D., Peck, W.D., Ayash, S.C., Melzer, L.S., Chatterjee, S., 2015. CO2 storage associated with CO2 enhanced oil recovery: a statistical analysis of historical operations. Int. J. Greenh. Gas Control 37, 384–397. https://doi.org/10.1016/j.ijggc.2015.03.037.
Bryant, S.L., Lakshminarasimhan, S., Pope, G.A., 2008. Buoyancy-dominated multiphase flow and its effect on geological sequestration of CO2. SPE J. 13, 447–454. https://doi.org/10.2118/99938-PA.
Buscheck, T.A., Bielicki, J.M., Edmunds, T.A., Hao, Y., Sun, Y., Randolph, J.B., Saar, M. O., 2016. Multifluid geo-energy systems: using geologic CO 2 storage for geothermal energy production and grid-scale energy storage in sedimentary basins. Geosphere 12, 678–696. https://doi.org/10.1130/GES01207.1.
Chamorro, C.R., Mondéjar, M.E., Ramos, R., Segovia, J.J., Martín, M.C., Villamañán, M. A., 2012. World geothermal power production status: energy, environmental and

economic study of high enthalpy technologies. 8th world energy system conference. WESC 42, 10–18. https://doi.org/10.1016/j.energy.2011.06.005, 2010.
Cui, G., Liang, Z., Ren, B., Enechukwu, C., Liu, Y., Ren, S., 2016. Geothermal exploitation from depleted high temperature gas reservoirs via recycling supercritical CO2: heat mining rate and salt precipitation effects. Appl. Energy 183, 837–852. https://doi.org/10.1016/j.apenergy.2016.09.029.
Cui, G., Ren, S., Rui, Z., Ezekiel, J., Zhang, L., Wang, H., 2018. The influence of complicated fluid-rock interactions on the geothermal exploitation in the CO2 plume geothermal system. Appl. Energy 227, 49–63. https://doi.org/10.1016/j.apenergy.2017.10.114.
Cui, Y., Zhu, J., Twaha, S., Chu, J., Bai, H., Huang, K., Chen, X., Zoras, S., Soleimani, Z., 2019. Techno-economic assessment of the horizontal geothermal heat pump systems: a comprehensive review. Energy Convers. Manag. 191, 208–236. https://doi.org/10.1016/j.enconman.2019.04.018.
Esteves, A.F., Santos, F.M., Pires, J.C.M., 2019. Carbon dioxide as geothermal working fluid: an overview. Renew. Sustain. Energy Rev. 114, 109331 https://doi.org/10.1016/j.rser.2019.109331.
Iglauer, S., 2017. CO_2 –Water–Rock wettability: variability, influencing factors, and implications for CO_2 geostorage. Accounts Chem. Res. 50, 1134–1142. https://doi.org/10.1021/acs.accounts.6b00602.
Isaka, B.A., Ranjith, P.G., Rathnaweera, T.D., Perera, M.S.A., Kumari, W.G.P., 2019. Influence of long-term operation of supercritical carbon dioxide based enhanced geothermal system on mineralogical and microstructurally-induced mechanical alteration of surrounding rock mass. Renew. Energy 136, 428–441. https://doi.org/10.1016/j.renene.2018.12.104.
Jiang, J., Rui, Z., Hazlett, R., Lu, J., 2019. An integrated technical-economic model for evaluating CO2 enhanced oil recovery development. Appl. Energy 247, 190–211. https://doi.org/10.1016/j.apenergy.2019.04.025.
Kabeyi, M., 2019. Geothermal electricity generation, challenges, opportunities and recommendations. International Journal of Advances in Scientific Research and Engineering 5, 53–95. https://doi.org/10.31695/IJASRE.2019.33408.
Kaya, E., Callos, V., Mannington, W., 2018. CO2 –water mixture reinjection into two-phase liquid dominated geothermal reservoirs. Renew. Energy 126, 652–667. https://doi.org/10.1016/j.renene.2018.03.067.
Lei, G., Yu, X., Li, T., Habibzadeh-Bigdarvish, O., Wang, X., Mrinal, M., Luo, C., 2020. Feasibility study of a New attached multi-loop CO2 heat pipe for bridge deck de-icing using geothermal energy. J. Clean. Prod. 275, 123160 https://doi.org/10.1016/j.jclepro.2020.123160.
Lei, Z., Zhang, Y., Yu, Z., Hu, Z., Li, L., Zhang, S., Fu, L., Zhou, L., Xie, Y., 2019. Exploratory research into the enhanced geothermal system power generation project: the Qiabuqia geothermal field, northwest China. Renew. Energy 139, 52–70. https://doi.org/10.1016/j.renene.2019.01.088.
Lei, Z., Zhang, Y., Zhang, S., Fu, L., Hu, Z., Yu, Z., Li, L., Zhou, J., 2020. Electricity generation from a three-horizontal-well enhanced geothermal system in the Qiabuqia geothermal field, China: slickwater fracturing treatments for different reservoir scenarios. Renew. Energy 145, 65–83. https://doi.org/10.1016/j.renene.2019.06.024.
Liao, J., Hu, K., Mehmood, F., Xu, B., Teng, Y., Wang, H., Hou, Z., Xie, Y., 2023. Embedded discrete fracture network method for numerical estimation of long-term performance of CO2-EGS under THM coupled framework. Energy 285, 128734. https://doi.org/10.1016/j.energy.2023.128734.
Lu, S., 2018. A global review of enhanced geothermal system (EGS). Renew. Sustain. Energy Rev. 81, 2902–2921. https://doi.org/10.1016/j.rser.2017.06.097.
Ma, H., McCoy, S., Chen, Z., 2022a. Economic and engineering Co-optimization of CO2 storage and enhanced oil recovery. SSRN scholarly paper. In: Proceedings of the 16th Greenhouse Gas Control Technologies Conference (GHGT-16). https://doi.org/10.2139/ssrn.4271583.
Ma, H., Yang, Y., Zhang, Y., Li, Z., Zhang, K., Xue, Z., Zhan, J., Chen, Z., 2022b. Optimized schemes of enhanced shale gas recovery by CO2-N2 mixtures associated with CO2 sequestration. Energy Convers. Manag. 268, 116062 https://doi.org/10.1016/j.enconman.2022.116062.
Norouzi, A.M., Babaei, M., Han, W.S., Kim, K.Y., Niasar, V., 2021. CO2 -plume geothermal processes: a parametric study of salt precipitation influenced by capillary-driven backflow. Chem. Eng. J. 425, 130031 https://doi.org/10.1016/j.cej.2021.130031.
Pruess, K., 2006. Enhanced geothermal systems (EGS) using CO2 as working fluid—a novel approach for generating renewable energy with simultaneous sequestration of carbon. Geothermics 35, 351–367. https://doi.org/10.1016/j.geothermics.2006.08.002.
Pruess, K., 2008. On production behavior of enhanced geothermal systems with CO2 as working fluid. Energy Convers. Manag. 49, 1446–1454. https://doi.org/10.1016/j.enconman.2007.12.029.
Salimi, H., Wolf, K.H., Bruining, J., 2012. Negative-saturation approach for compositional flow simulations of mixed CO2/water injection into geothermal reservoirs including phase appearance and disappearance. SPE J. 17, 502–522. https://doi.org/10.2118/142924-PA.
Shi, Y., Song, X., Li, J., Wang, G., Zheng, R., YuLong, F., 2019a. Numerical investigation on heat extraction performance of a multilateral-well enhanced geothermal system with a discrete fracture network. Fuel 244, 207–226. https://doi.org/10.1016/j.fuel.2019.01.164.
Shi, Y., Song, X., Shen, Z., Wang, G., Li, X., Zheng, R., Geng, L., Li, J., Zhang, S., 2018. Numerical investigation on heat extraction performance of a CO2 enhanced geothermal system with multilateral wells. Energy 163, 38–51. https://doi.org/10.1016/j.energy.2018.08.060.
Shi, Y., Song, X., Wang, G., McLennan, J., Forbes, B., Li, X., Li, J., 2019b. Study on wellbore fluid flow and heat transfer of a multilateral-well CO2 enhanced geothermal system. Appl. Energy 249, 14–27. https://doi.org/10.1016/j.apenergy.2019.04.117.
Singh, M., Mahmoodpour, S., Ershadnia, R., Soltanian, M.R., Sass, I., 2023. Comparative study on heat extraction from soultz-sous-forêts geothermal field using supercritical carbon dioxide and water as the working fluid. Energy 266, 126388. https://doi.org/10.1016/j.energy.2022.126388.
Soltani, M., Kashkooli, F.M., Souri, M., Rafiei, B., Jabarifar, M., Gharali, K., Nathwani, J. S., 2021. Environmental, economic, and social impacts of geothermal energy systems. Renew. Sustain. Energy Rev. 140, 110750 https://doi.org/10.1016/j.rser.2021.110750.
Song, X., Guo, Y., Zhang, J., Sun, N., Shen, G., Chang, X., Yu, W., Tang, Z., Chen, W., Wei, W., Wang, L., Zhou, J., Li, X., Li, X., Zhou, J., Xue, Z., 2019. Fracturing with carbon dioxide: from microscopic mechanism to reservoir application. Joule 3, 1913–1926. https://doi.org/10.1016/j.joule.2019.05.004.
Sowiżdżał, A., Machowski, G., Krzyżak, A., Puskarczyk, E., Krakowska-Madejska, P., Chmielowska, A., 2022. Petrophysical evaluation of the lower permian formation as a potential reservoir for CO2 - EGS – case study from NW Poland. J. Clean. Prod. 379, 134768 https://doi.org/10.1016/j.jclepro.2022.134768.
Tagliaferri, M., Gładysz, P., Ungar, P., Strojny, M., Talluri, L., Fiaschi, D., Manfrida, G., Andresen, T., Sowiżdżał, A., 2022. Techno-economic assessment of the supercritical carbon dioxide enhanced geothermal systems. Sustainability 14, 16580. https://doi.org/10.3390/su142416580.
Xie, J., Wang, J., 2022. Compatibility investigation and techno-economic performance optimization of whole geothermal power generation system. Appl. Energy 328, 120165. https://doi.org/10.1016/j.apenergy.2022.120165.
Xu, T., Feng, G., Shi, Y., 2014. On fluid–rock chemical interaction in CO2-based geothermal systems. J. Geochem. Explor. 144, 179–193. https://doi.org/10.1016/j.gexplo.2014.02.002.
Xu, J., Wu, K., Li, R., Li, Z., Li, J., Xu, Q., Chen, Z., 2018. Real gas transport in shale matrix with fractal structures. Fuel 219, 353–363. https://doi.org/10.1016/j.fuel.2018.01.114.
Xu, Y., Hu, J., Wang, Y., Zhang, W., Wu, W., 2022. Understanding the economic responses to China's electricity price-cutting policy: evidence from zhejiang province. Sustainability 14, 11701. https://doi.org/10.3390/su141811701.
Xue, Z., Ma, H., Chen, Z., 2023. Numerical investigation of energy production from an enhanced geothermal system associated with CO2 geological sequestration. In: SPE Western Regional Meeting.
Xue, Z., Chen, Z., 2023a. Deep learning based production prediction for an enhanced geothermal system (EGS). In: SPE Canadian Energy Technology Conference. https://doi.org/10.2118/212754-MS.
Xue, Z., Yao, S., Ma, H., Zhang, C., Zhang, K., Chen, Z., 2023b. Thermo-economic optimization of an enhanced geothermal system (EGS) based on machine learning and differential evolution algorithms. Fuel 340, 127569. https://doi.org/10.1016/j.fuel.2023.127569.
Xue, Z., Zhang, K., Zhang, C., Ma, H., Chen, Z., 2023c. Comparative data-driven enhanced geothermal systems forecasting models: a case study of Qiabuqia field in China. Energy 280, 128255. https://doi.org/10.1016/j.energy.2023.128255.
Xue, Z., Ma, H., Wei, Y., Wu, W., Sun, Z., Chai, M., Zhang, C., Chen, Z., 2024. Integrated technological and economic feasibility comparisons of enhanced geothermal systems associated with carbon storage. Appl. Energy 359, 122757. https://doi.org/10.1016/j.apenergy.2024.122757.
Yang, Y., Clarkson, C.R., Hamdi, H., Ghanizadeh, A., Blinderman, M.S., Evans, C., 2023. Field pilot testing and reservoir simulation to evaluate processes controlling CO2 injection and associated in-situ fluid migration in deep coal. Int. J. Coal Geol. 275, 104317 https://doi.org/10.1016/j.coal.2023.104317.
Yang, Y., Liu, S., Ma, H., 2024. Impact of unrecovered shale gas reserve on methane emissions from abandoned shale gas wells. Sci. Total Environ. 913, 169750 https://doi.org/10.1016/j.scitotenv.2023.169750.
Yu, P., Dempsey, D., Archer, R., 2022. Techno-economic feasibility of enhanced geothermal systems (EGS) with partially bridging multi-stage fractures for district heating applications. Energy Convers. Manag. 257, 115405 https://doi.org/10.1016/j.enconman.2022.115405.
Zhang, L., Ezekiel, J., Li, D., Pei, J., Ren, S., 2014. Potential assessment of CO2 injection for heat mining and geological storage in geothermal reservoirs of China. Appl. Energy 122, 237–246. https://doi.org/10.1016/j.apenergy.2014.02.027.
Zhang, L., Cui, G., Zhang, Y., Ren, B., Ren, S., Wang, X., 2016. Influence of pore water on the heat mining performance of supercritical CO2 injected for geothermal development. J. CO2 Util. 16, 287–300. https://doi.org/10.1016/j.jcou.2016.08.008.
Zhang, C., Jiang, G., Jia, X., Li, S., Zhang, S., Hu, D., Hu, S., Wang, Y., 2019. Parametric study of the production performance of an enhanced geothermal system: a case study at the Qiabuqia geothermal area, northeast Tibetan plateau. Renew. Energy 132, 959–978. https://doi.org/10.1016/j.renene.2018.08.061.
Zhao, Y., Diao, H., Qin, Y., Xie, L., Ge, M., Wang, Y., Wang, S., 2023. Effect of flow rate on condensation of CO2-water vapor mixture on a vertical flat plate. Appl. Therm. Eng. 229, 120557 https://doi.org/10.1016/j.applthermaleng.2023.120557.